



# Preparation of magnesium diniobate by solid–state reactions and its role for hydrogen storage

Md. Wasikur Rahman<sup>1,2</sup>

Received: 16 November 2017 / Revised: 15 June 2018 / Accepted: 23 September 2018 / Published online: 25 October 2018  
© Australian Ceramic Society 2018

## Abstract

A ternary compound of magnesium diniobate ( $\text{MgNb}_2\text{O}_6$ ) was prepared by solid–state reactions in order to understand the role of transition metal oxides as a promoter/catalyst for hydrogen storage in Mg/MgH<sub>2</sub> systems.  $\text{MgNb}_2\text{O}_6$  was prepared in almost pure form in oxidizing conditions by annealing a stoichiometric mixture of MgO and Nb<sub>2</sub>O<sub>5</sub>. The effect of calcination temperatures on phase formation, reaction kinetics, and heat of reaction of the solid–state product was investigated by ex situ, in situ X-ray diffraction (XRD), and differential scanning calorimetry (DSC). Hydrogen sorption properties of the compound were investigated by mass spectrometer. The crystallographic parameters of binary and ternary Mg–Nb–O phases were extracted by Rietveld method. During solid–state synthesis, the formation of  $\text{MgNb}_2\text{O}_6$  provides single-step reaction between precursor materials proved by in situ experiment and the heat of formation as well as driving force was calculated from calorimetric analysis.

**Keywords** Solid–state synthesis · Magnesium diniobate · X-ray techniques · Reaction kinetics · Rietveld refinement

## Introduction

Current increase in catalytic application of transition metal oxides, especially, ternary Mg–Nb oxides for solid–state hydrogen storage systems, draws attention to the researchers with a great extent. It was reported that milling MgH<sub>2</sub> with Nb<sub>2</sub>O<sub>5</sub> influences the sorption kinetics of the system by the formation of ternary Mg–Nb–O compounds during the hydrogen sorption cycles [1–5]. Friedrichs et al. [6] proposed a reactive pathway model, explained by the successive reduction of Nb<sub>2</sub>O<sub>5</sub> into metallic Nb, together with a simultaneous formation of ternary Mg–Nb oxides of various stoichiometries at the interfaces with the MgH<sub>2</sub> phase, facilitating hydrogen transport into the solid structure.

In addition, the columbite-like phase of  $\text{MgNb}_2\text{O}_6$  has attracted interest for many years [7–10] with current attention tending to focus on its use in the synthesis of microwave dielectric materials e.g.,  $\text{Ba}(\text{Mg}_{1/3}\text{Nb}_{2/3})\text{O}_3$  [11].  $\text{MgNb}_2\text{O}_6$  is well known as the key precursor for the preparation of single phase perovskite  $\text{Pb}(\text{Mg}_{1/3}\text{Nb}_{2/3})\text{O}_3$ , successively increasing its demand for multilayer ceramic capacitor, transducer, electrostrictor, and actuator applications [12–14]. It is also a suitable reference material for investigating the defects induced in LiNbO<sub>3</sub> substrates for waveguide fabrication [15].

The state-of-the-art technology of the preparation of semiconductor/semiconductor hetero-junctions with enhanced luminescence and conductive properties is still a challenge [16, 17]. The photoluminescence behavior of nanostructured materials not only depends on the structure but also is controlled by surface chemical bonding and optical transitions in the region of the surface/interface [18, 19].  $\text{MgNb}_2\text{O}_6$  is a luminescent material. Figure 1 shows a schematic presentation of the  $\text{MgNb}_2\text{O}_6$  crystal ( $1 \times 1 \times 1$ ) unit cells with clusters. A unit cell for  $\text{MgNb}_2\text{O}_6$  crystal with a columbite-type orthorhombic structure has been illustrated in the figure with a space group of (*pbcn*) and point–group symmetry (*D*<sub>2h</sub>). In this unit cell, magnesium atoms (Mg) and niobium (Nb) atoms are coordinated to six oxygen (O) atoms which form distorted octahedral [ $\text{MgO}_6$ ]/[ $\text{NbO}_6$ ] clusters [20]. These octahedra are formed by 6 vertices, 6 faces, and 12 edges. XRD is a valuable

**Electronic supplementary material** The online version of this article (<https://doi.org/10.1007/s41779-018-0265-5>) contains supplementary material, which is available to authorized users.

✉ Md. Wasikur Rahman  
mwrahman.ump@gmail.com

<sup>1</sup> Department of Chemical Engineering, Jessore University of Science and Technology, Jessore 7408, Bangladesh

<sup>2</sup> Faculty of Chemical and Natural Resources Engineering, Universiti Malaysia Pahang, Gambang, 26300 Kuantan, Malaysia

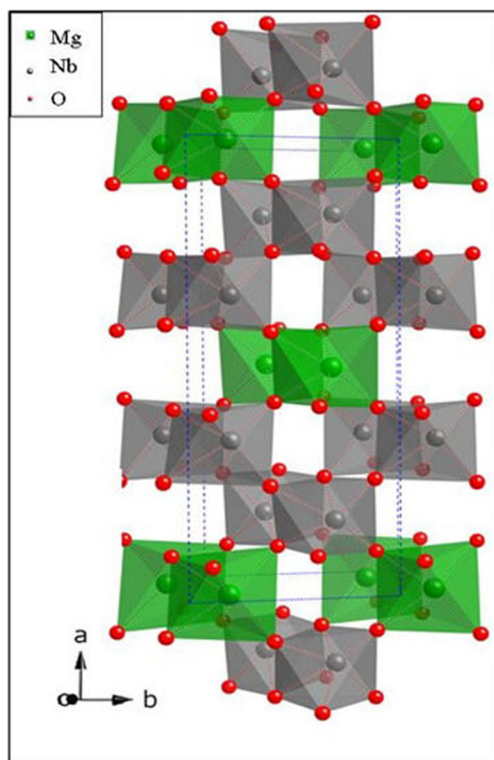


**Fig. 1** Schematic presentation of the unit cells of  $\text{MgNb}_2\text{O}_6$  crystal. The picture is drawn with a relatively close perspective

tool to identify the crystallographic parameters of microstructures.

A number of chemical routes were explored for the synthesis of ternary Mg–Nb–O compounds by using expensive precursors, high calcination temperature (1373–1573 K) and long calcination time (up to 48 h) by a conventional mixed oxide synthetic route, though no details on phase formation were provided [21–24]. Furthermore, Saha et al. [13] reported effective attempts to prepare solid-state-derived  $\text{MgNb}_2\text{O}_6$  powder followed by re-grinding and re-calcination processes. Pagola et al. [24] described a conventional solid-state reaction method for the synthesis of ternary Mg–Nb oxides, based on a simple annealing of commercially available precursor materials. The synthesis of  $\text{MgNb}_2\text{O}_6$  phase, derived from the reaction of binary oxides, usually results in varying amount of the corundum-like  $\text{Mg}_4\text{Nb}_2\text{O}_9$  phase alongside the columbite-like  $\text{MgNb}_2\text{O}_6$  phase [25]. Crystallographic, microstructural, and morphological studies of  $\text{MgNb}_2\text{O}_6$  compound, formed by solid-state reactions, were investigated by Sun et al. [26]. However, all dealings were qualitative point of view. On the basis of current knowledge, only Dolci et al. [27] made an attempt to quantify  $\text{MgNb}_2\text{O}_6$  preparation by Rietveld method; nevertheless, the group obtained multiple Mg–Nb–O binary/ternary phases instead of the unique phase. Therefore, systematic investigation of  $\text{MgNb}_2\text{O}_6$  compound with reaction kinetics perspective and to elucidate a possible role of

the ternary compound regarding hydrogen uptake/release in  $\text{MgH}_2$  system is to date lacking.

The aim of this work is to explore comprehensively a synthetic route for the preparation of pure  $\text{MgNb}_2\text{O}_6$  phase using solid-state reactions between the starting MgO and  $\text{Nb}_2\text{O}_5$  materials and crystallographic parameters of binary and ternary Mg/Nb/O phases were evaluated.

## Experimental

The starting materials used for the solid-state synthesis of  $\text{MgNb}_2\text{O}_6$  were commercially available magnesium oxide (MgO) and niobium(V) oxide ( $\text{Nb}_2\text{O}_5$ ) (Sigma-Aldrich, 99% purity). It was prepared by annealing the accurate molar ratio of MgO/ $\text{Nb}_2\text{O}_5$  (1:1) powders in oxidizing environment. The mixtures of the parent materials were heated at different temperatures, e.g., room temperature (RT), 473, 673, 873, 1073, 1273, and 1473 K for 24 h with a heating rate of 5 K/min. The structure of as-prepared materials has been analyzed by ex situ XRD at RT with an X'Pert diffractometer (Panalytical) with  $\text{Cu K}\alpha$  radiation.

In situ XRD was performed using a hot stage and environmental chamber (Anton Paar XRD 900). XRD patterns were collected in a  $0.017^\circ$  step for 6 min in isothermal condition from RT to 1173 K at 20 K/min with suitable temperature step programs. The experiment was done under vacuum using steel sample holder for cumulative time 10 h, requiring each step for 2 h. The thermal expansion of the steel sample holder has been estimated with a sample of  $\alpha$ -quartz and it brings to an angle shift of about  $0.1^\circ$ . On the other hand, the observed peak shift cannot account for the thermal expansion of the crystalline phases; which would bring to a limited variation of the lattice constants. So, it is considered that during synthetic experiments, the powder sample surface moves significantly from the centre of the goniometer. A continuous rotary vacuum was introduced into the chamber and 20 diffraction patterns were recorded for each temperature step as a function of time and then averaged. Structural features were analyzed by MAUD (material analysis using diffraction), a general diffraction/reflectivity analysis program mainly based on Rietveld method [28].

Differential scanning calorimetry (DSC) data were recorded from RT to 1473 K at a heating rate of 5 K/min by successive flow of He and Ar using a high temperature DSC Setaram. The mixture of starting materials and the reference ( $\alpha\text{-Al}_2\text{O}_3$ ) of  $\sim 200$  mg each were loaded in Pt crucibles. It is possible to determine the heat of formation of the compound on the basis of calorimetric signals.

Hydrogen storage properties were investigated by thermal programmed desorption (TPD) coupled with a home-made heating apparatus to a quadrupolar mass spectrometer (MS, Pfeiffer Vacuum Prisma). Desorption data was recorded

during TPD measurements between 298 and 1073 K with a heating rate of 10 K/min in ultra vacuum ( $10^{-6}$  bar) condition. All samples were degassed at RT and then the thermal desorption runs were done. The cleaned sample was then contacted with molecular hydrogen ( $P_{H_2} = 150$  mbar) for absorption at 673 K for 30 min followed by desorption in the previous conditions.

## Results and discussion

### Ex situ experiment

In order to understand the gradual phase evolution with temperatures during heating of the precursor materials towards the target pure  $MgNb_2O_6$ , ex situ XRD patterns were recorded in the range from RT to 1473 K with intervals of 200 K. All diffraction patterns were recorded in the range from  $10^\circ$  to  $90^\circ$ ; however, for the sake of simplicity, only the data from 20 to  $50^\circ$  are reported. The solid-state phase developed en route for the pure ternary oxide is assigned by ICSD databases and the quality of refinement ( $R < 3\%$ ) is excellent. XRD patterns are shown in Fig. 2 (a–g), and corresponding phase evolution during the preparation obtained by Rietveld analysis is reported in Table 1. Two forms of crystal structures were observed for the precursor niobia (monoclinic, MC and orthorhombic, OR); of them, MC  $Nb_2O_5$  was abundant and more stable because at higher temperatures ( $> 873$  K), almost all OR  $Nb_2O_5$  was converted to MC (Table 1).

During the synthesis, the theoretical MgO and  $Nb_2O_5$  were required (1:1 M ratio); 13.17 and 86.83 wt% were very close to our results obtained from Rietveld refinement inserted in

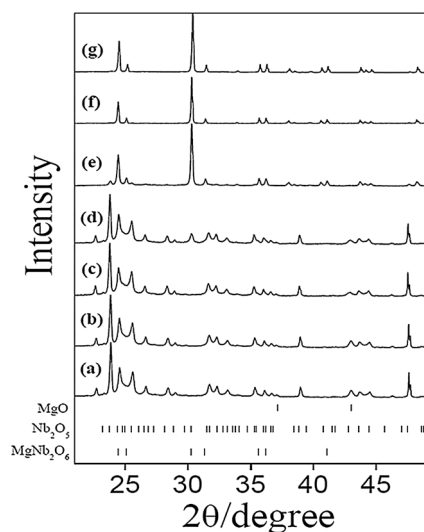


**Fig. 2** Ex situ XRD patterns recorded at room temperature during  $MgNb_2O_6$  preparation annealed for 24 h at various temperatures: (a) 298 K, (b) 473 K, (c) 673 K, (d) 873 K, (e) 1073 K, (f) 1273 K, and (g) 1473 K

**Table 1** Abundance of  $MgNb_2O_6$  during ex situ measurements obtained by Rietveld refinement. MC = monoclinic, OR = orthorhombic,  $O_6 = MgNb_2O_6$ .

T/K	Phase composition (wt% $\pm 2$ )				R%
	$Nb_2O_5$ MC	$Nb_2O_5$ OR	MgO	$O_6$	
298	80	7	13	0	2.45
473	81	7	12	0	2.38
673	78	6	7	9	2.40
873	67	5	4	24	1.80
1073	20	0	0	80	1.36
1273	10	0	0	90	1.48
1473	3	0	0	97	1.86

Table 1. The phase quantities of precursor materials were decreasing, whereas that of the desired  $MgNb_2O_6$  phase (ICSD 01–088–0708, space group *pbcn*,  $a = 14.194$  Å,  $b = 5.703$  Å, and  $c = 5.039$  Å) [4, 24, 25] was increasing with a little discrimination in the results; however,  $\pm 2\%$  error can be accepted for Rietveld refinement.

Throughout the synthesis, no solid-state reactions between the binary oxides (cubic MgO and MC  $Nb_2O_5$ ) took place from RT to less than 673 K during milling process (Fig. 2 (a, b)) [25]. A small amount of  $MgNb_2O_6$  phase was appeared ( $\sim 9$  wt%) at calcination temperature of 673 K (Fig. 2 (c)). The phase evolution was also reported in the literatures at 873–923 K [22] and 773 K [25] at a heating rate of 10 K/min, still higher than the present study. The effect of heating rates (5–10 K/min) might be showed discrimination in the results.

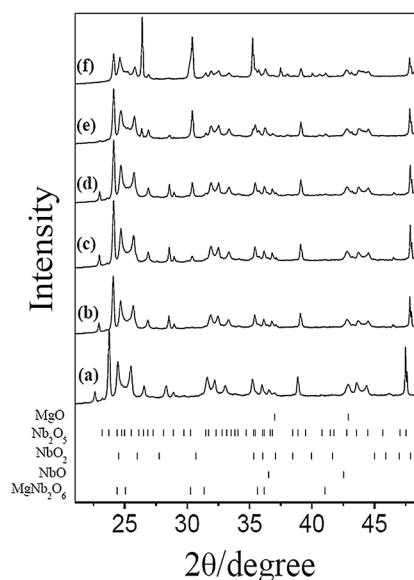


**Fig. 3** In situ XRD patterns recorded during  $MgNb_2O_6$  preparation in isothermal condition at a heating rate of 20 K/min at various temperatures: (a) 298 K, (b) 973 K, (c) 1023 K, (d) 1073 K, (e) 1123 K, and (f) 1173 K

However, the phase development with increasing heating/cooling rates ranging from 10 to 30 K/min did not vary significantly [25]. Then, the quantity of magnesium diniobate was grown up (~24 wt%) at 873 K (Fig. 2 (d)) according to the following reaction (Reaction 1):



As the temperature was increased to 1073 K, the intensity of the columbite-like  $\text{MgNb}_2\text{O}_6$  phase became predominant (Fig. 2 (e)) and at 1273 K a nearly pure  $\text{MgNb}_2\text{O}_6$  phase (~90 wt%) excepting traces of unreacted  $\text{Nb}_2\text{O}_5$  (Fig. 2 (f)) was appeared. The formation of the ternary phase was almost completed (~97 wt%) at 1473 K (Fig. 2 (g)). Ananta [25] also reported that there were no significant differences between the powders calcined at temperature ranging from 1273 to 1473 K as observed in the present study. Dolci et al. [27] synthesized  $\text{MgNb}_2\text{O}_6$  by solid–state reactions at 1273 K for 32 h, and the crystallographic parameters were analyzed by Rietveld refinement. The group obtained only 26.30 wt%  $\text{MgNb}_2\text{O}_6$  alongside 45.80 and 22.70 wt%  $\text{Mg}_4\text{Nb}_2\text{O}_9$  and  $\text{Mg}_3\text{Nb}_6\text{O}_{11}$  phases, respectively and the balance  $\text{NbO}_x$ . In fact, the solid product is always contaminated with unreacted  $\text{Nb}_y\text{O}_x$  may be due to poor activity of Mg and Nb species [12, 29]. It is rather interesting that no evidence of the corundum  $\text{Mg}_4\text{Nb}_2\text{O}_9$  [29, 30] was found in this study nor was there any indication of the  $\text{Mg}_5\text{Nb}_4\text{O}_{15}$  [24] being present thanks to controlled reaction conditions. As a result,  $\text{MgNb}_2\text{O}_6$  preparation in almost pure form at the calcination temperature and dwell time observed in this work were also lower than those reported earlier [14, 30, 31]. It is well documented that powder prepared by conventional mixed oxide method has spatial fluctuations in their compositions. The extent of the fluctuation depends on the characteristics of the precursors as well as the processing schedules [12, 13, 30].

### In situ experiment

For kinetic study, in situ XRD patterns of the ternary phase ( $\text{MgNb}_2\text{O}_6$ ) evolution as a function of time are shown in Fig. 3 (a–f) and the corresponding phase profusion obtained by Rietveld refinement is inserted in Table 2. The first pattern (Fig. 3 (a)) was recorded at RT to be considered as a reference for the others. The temperature increased to 973 K and resided for 2 h; no change in precursor materials was observed (Fig. 3 (b)) that proved the lower rate of reaction between precursors as reported elsewhere [12, 29]. Then, successive four steps of 50 K intervals were carried out requiring each step for 2 h. A trace amount of NbO (II) formed by reducing Nb (V) oxide at 1023 K and  $\text{MgNb}_2\text{O}_6$  just started to form at 1073 K (Fig. 3 (c, d)) according to the Reaction 1, and its abundance increased

**Table 2** Abundance of  $\text{MgNb}_2\text{O}_6$  during in situ measurements in isothermal conditions from RT to 1173 K at a heating rate of 20 K/min with suitable step programs, obtained by Rietveld refinement. MC = monoclinic, OR = orthorhombic,  $\text{O}_6$  =  $\text{MgNb}_2\text{O}_6$

T/K	Phase composition (wt% ± 2)						R%
	$\text{Nb}_2\text{O}_5$ MC	$\text{Nb}_2\text{O}_5$ OR	NbO	$\text{NbO}_2$	MgO	$\text{O}_6$	
298	79	9	0	0	12	0	1.60
973	78	9	0	0	13	0	1.54
1023	77	8	2	0	13	0	1.44
1073	77	9	2	0	11	1	1.50
1123	73	0	0	5	9	13	1.37
1173	55	0	0	17	8	20	1.33

with temperature as observed for the ex situ measurement [25].

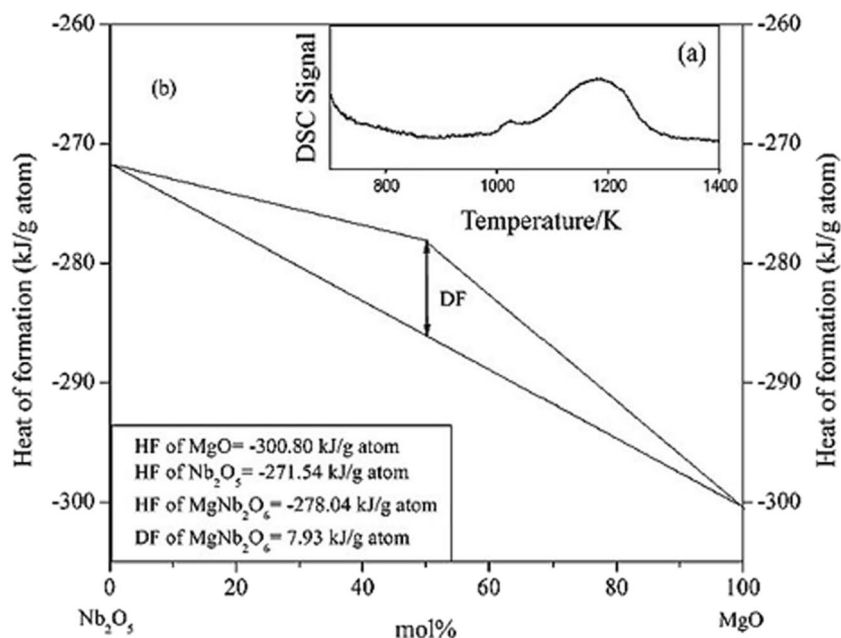
Nielsen et al. [32] investigated  $\text{MgH}_2$ – $\text{Nb}_2\text{O}_5$  system by in situ synchrotron XRD and showed that at elevated temperatures, Nb (II) was reduced to metallic Nb (0) and extracted from the ternary oxide ( $\text{Mg}_x\text{Nb}_{1-x}\text{O}$ ) and formed in a reaction with Mg. In the present work, Nb (0) was unidentified probably owing to highly reactive surface of transition metals might be oxidized immediately with other oxides present in the system. Then, the starting materials began to reduce and the desired phase produced (~13 wt%) along with some  $\text{NbO}_2$  at 1123 K (Fig. 3 (e)) [27]. About 20 wt%,  $\text{MgNb}_2\text{O}_6$  phase was grown up at 1173 K in dynamic isothermal heat treatment (Fig. 3 (f)). Results give us valuable information about how fast the precursor materials react to form the ternary Mg–Nb–O compound.

There was some discrimination with this kind of approach to the ex situ results. No pure phases were obtained in this case, due to the facts related; first of all, the maximum possible temperature reached with the apparatus employed (1173 K) is lower than the temperatures applied in the ex situ preparation (1473 K). Secondly, it is due to the lower reaction time with respect to the ex situ experiments. Nevertheless, this set of data is in good agreement with those obtained with the previous method and the following considerations can be counted:

During ex situ measurement, no appreciable reaction took place between parent materials at relatively low temperatures (< 673 K). In contrast, during in situ experiment, the reaction temperature was directly increased up to 973 K, prior to this measurement, an initial pattern recorded at RT. Another relevant difference between ex situ and in situ experiments was the formation in this second case of lower valences niobium oxides ( $\text{NbO}$  (+2) and  $\text{NbO}_2$  (+4)). Considering that NbO and MgO show a NaCl structure with a very similar lattice parameter, therefore, the bond lengths between metal and oxygen atoms in MgO, NbO, and  $\text{NbO}_2$  phases are comparable; a reaction between the niobium oxide and the Mg/MgH<sub>2</sub> with



**Fig. 4** (a) DSC curve of  $\text{MgNb}_2\text{O}_6$  with respect to temperature from RT to 1473 K (only significant portion shown) at a heating rate of 5 K/min and (b) driving force (DF) estimated (7.93 kJ/g atom) from heat of formation (HF) of  $\text{MgNb}_2\text{O}_6$  (–278.04 kJ/g atom) calculated on the basis of that of precursor materials  $\text{MgO}$  and  $\text{Nb}_2\text{O}_5$  of molar ratio 1:1



a formation of a ternary oxide  $\text{Mg}_x\text{Nb}_y\text{O}$  was reported by Friedrich et al. [33]. The presence of this kind of compounds ( $\text{NbO}$ ,  $\text{NbO}_2$ ) could be explained considering that the in situ experiments were carried out in static vacuum condition which favored the formation of lower niobium oxidation states (Reaction 2) [27, 33].



The results obtained by ex situ and in situ show that about 24 wt%  $\text{MgNb}_2\text{O}_6$  phase was formed at 873 K in the first case (Table 1), whereas during in situ measurement, the same amount of the phase was formed at higher temperature of 1173 K (Table 2), indicating that  $\text{MgNb}_2\text{O}_6$  formation was

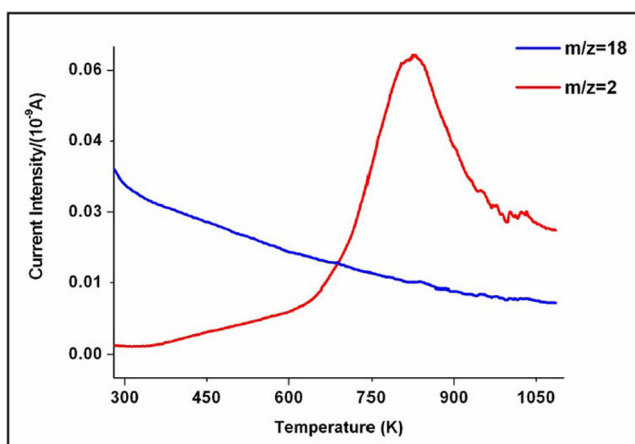


**Fig. 5** TPD-MS spectra of  $\text{MgNb}_2\text{O}_6$  after treatment with molecular  $\text{H}_2$  at 673 K. Red curve shows  $\text{H}_2$  desorption, and blue one corresponds to water desorption peaks

promoted by the oxidizing ambient and calcination conditions [25, 27].

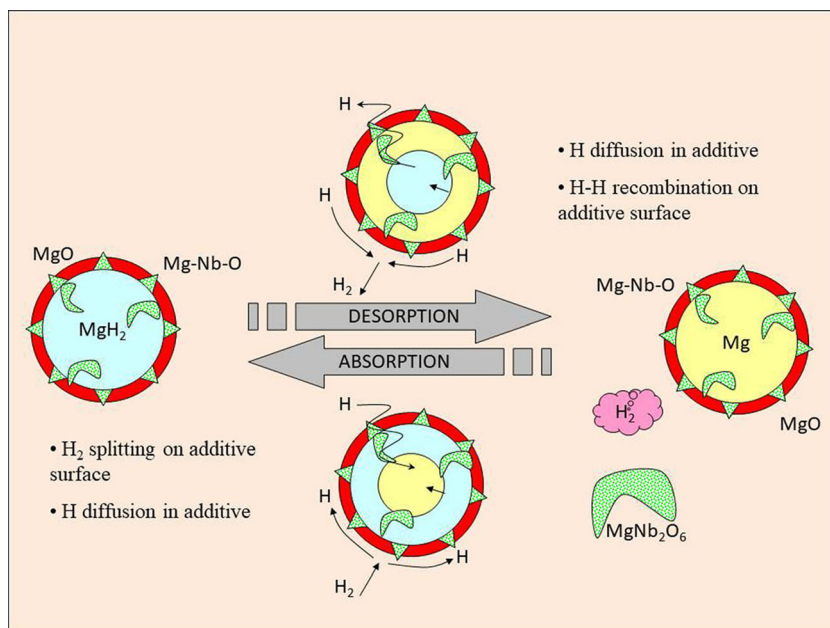
## DSC experiment

$\text{MgNb}_2\text{O}_6$  preparation was studied by DSC in order to unambiguously assign the observed heat of reaction to the ternary compound. Figure 4 (a) demonstrates the DSC measurement of annealing the parent materials from 950 to 1400 K (only the significant portion shown). The curve was characterized by two exothermic signals centered at about 1090 and 1180 K that suggest that the overall process leading to the synthesis is more complex rather the simple reaction (Reaction 1). Two DSC signals regarding at least two step reactions could be interpreted considering the following two aspects.

Firstly, the heating process involved in the DSC measurement is very similar to the in situ experiment where the heat treatment was done in the absence of oxygen. In situ results also indicates that reaction involved in the  $\text{MgNb}_2\text{O}_6$  preparation in the absence of oxygen is kinetically less favored and the formation of intermediates as  $\text{NbO}$  and  $\text{NbO}_2$  [27] in the range 1023–1173 K is observed. Reaction 1 was possibly carried out in this step (wider peak). Secondly, the formation of such intermediates could also be invoked during DSC measurement to explain the lower peak in the DSC curve. Similar results were also explained by Jin et al. [34] for  $\text{NbF}_5$ -added  $\text{MgH}_2$  system. In this specific case, however, they further reacted at higher temperatures [32, 33] since they were not present in the final product, examined by XRD analysis. The solid product obtained after DSC was almost pure.

The heat of formation of  $\text{MgNb}_2\text{O}_6$  by solid–state reaction was estimated from the calorimetric curve (Fig. 4 (b)). The

**Fig. 6** Schematic presentation of a kinetic model showing  $H_2$  storage mechanism through the MgO layer by crafting a pathway of Mg–Nb–O additive during  $H_2$  sorption



heat of formation of pure  $Nb_2O_5$  and MgO is  $-271.54$  and  $-300.80$  kJ/g atom, respectively, obtained from available databases [35] and that of  $MgNb_2O_6$  has been calculated to be  $-278.04$  kJ/g atom. On the basis of this database, it is also possible to obtain driving force for the formation of the ternary compound and found to be  $\sim 7.93$  kJ/g atom (Fig. 4 (b)) as of the deviation of calculated value to that at 50 mol% (1:1 M ratio) of the pure constituents shown in the figure. Not much reported in the literature concerning driving force calculation from the solid-state synthesis of Mg–Nb oxides. Rahman et al. [5] estimated the thermodynamic and kinetic effects of hydrogen sorption in  $MgH_2$ , and the driving forces for hydrogen absorption and desorption in Mg were calculated. For a prescribed temperature and pressure, a driving force of about 10 kJ/mol  $H_2$  was obtained. The phenomenon is a little bit far from the present study; however, both used the graphical method based on thermodynamic databases.

### TPD-MS measurement

A tentative TPD-MS measurement of  $MgNb_2O_6$  sample was carried out in order to understand its behavior with respect to  $H_2$  uptake/release (Fig. 5). During the experiment, clean magnesium diniobate compound was interacted with molecular  $H_2$  and the TPD plot showed  $H_2$  desorption peak (red color) centered at about 825 K of higher intensity in comparison to that related to water desorption (blue color). The binary oxides employed as starting materials (MgO and  $Nb_2O_5$ ) contain physisorbed water and surface hydroxyl groups which cannot be removed completely by simple degassing at RT. This may cause desorption of water during the synthesis which oxidizes the highly reactive metallic niobium, producing molecular

hydrogen which remains trapped in the solid structure. The reversible interaction of hydrogen with  $MgNb_2O_6$  can be tentatively explained in terms of an original structural feature (columbite-type orthorhombic) of the solid (Fig. 1). Nonetheless, to estimate the actual hydrogen storage capacity of the ternary compound is rather complicated owing to hydroxyl groups (OH) present on the surface like precursor materials explained earlier. In addition, the amount of hydrogen absorbed due to the Mg–Nb–O phase is lower than the maximum stoichiometric capacity of  $MgH_2$  (7.6 wt%) because of the presence of a non-reactive MgO layer on the surface of the powders or at the grain boundaries.

In fact, the hydrogen desorption peak occurred at a temperature higher than that adopted for  $H_2$  storage in the real  $MgH_2/Nb_2O_5$  system [5, 27]. This may be due to low  $H_2$  pressure adopted in our study (150 mbar) and to the fact that the materials obtained after synthesis are composed of sintered particles which are not nanocrystalline in nature, like those formed under the mechanical action during ball-milling [36].

### $H_2$ storage mechanism

The role of ternary Mg–Nb oxides on  $H_2$  absorption and desorption properties of  $MgH_2$  has been discussed on the basis of kinetic model explained by the formation of reactive pathways of the ternary oxide with easier splitting of  $H_2$  that facilitate  $H_2$  transport into the solid structure. The schematic diagram of  $H_2$  ab/desorption in  $MgH_2$  is shown in Fig. 6. The kinetic model can be explained by three key steps: dissociation of molecular hydrogen into H atoms, diffusion of H into Mg to form  $MgH_2$  during adsorption, and successive

recombination of H–H on the surface of the ternary oxide during desorption makes a trap for H<sub>2</sub> sorption in the system.

In general, decomposition of MgH<sub>2</sub>, simultaneously formation of Mg (MgH<sub>2</sub> → Mg + H<sub>2</sub>), takes place via desorption process and hydrogenation of Mg (Mg + H<sub>2</sub> → MgH<sub>2</sub>) occurs by means of absorption process. A non-permeable MgO barrier is always present in the samples due to minor oxidation during nanostructuring. Ternary Mg–Nb–O additive is the key tool to overcome the H<sub>2</sub> hindrance by easier penetration of H inside. The diffusion of H<sub>2</sub> through Mg shell is initially faster and H atoms rapidly reach at the surface of the particles, and gradually reaction kinetics reduces due to contaminated interface [37, 38]. The MgNb<sub>2</sub>O<sub>6</sub> additive forms bonds with H; hydrogen diffuses inside and allows easier recombination of H–H towards the molecular state.

Rahman M.W. [39] explained some possibilities of the prominent effect of Mg–Nb–O additive on the H<sub>2</sub> storage of MgH<sub>2</sub> as follows: (i) the additive segregates at the grain boundaries during ball milling and thus increases both H diffusion along the boundaries and H–H recombination on the additive surface; (ii) pathways of Mg–Nb oxide might be formed by incorporating into MgH<sub>2</sub> structures during H<sub>2</sub> interaction, which would enhance the atomic hydrogen diffusion from the surface to bulk MgH<sub>2</sub>; and (iii) dispersion of additives might aid ball milling of MgH<sub>2</sub> to obtain nanoparticles that shorten the diffusion path.

## Conclusion

In order to obtain a clear understanding of the role of transition metal oxides as a promoter/catalyst during hydrogen absorption/desorption cycles in MgH<sub>2</sub>, pure MgNb<sub>2</sub>O<sub>6</sub> has been synthesized by solid–state reactions. The as-prepared materials were characterized by ex situ and in situ XRD and DSC analyses and H<sub>2</sub> sorption properties were examined by TPD-MS measurement. The synthetic reaction of the ternary compound showed single-step reaction with some intermediates of niobium oxides examined by in situ XRD and DSC experiments. All XRD results were evaluated by Rietveld analysis. The heat of formation and driving force of the compound was calculated on the basis of available thermodynamic databases. The synthetic approach of two other ternary solids (Mg<sub>4</sub>Nb<sub>2</sub>O<sub>9</sub> and Mg<sub>3</sub>Nb<sub>6</sub>O<sub>11</sub>) including the real system of Mg/MgH<sub>2</sub> is also under consideration for the same in the upcoming issues.

**Acknowledgements** Special thanks to Professor Marcello Baricco for technical assistance.

**Funding information** This work is financially granted by the Ministry of Education, Universities and Research (MIUR), Italy.

## References

- Friedrich, O., Aguey-Zinsou, F., Fernandez, J.R.A., Sanchez-Lopez, J.C., Justo, A., Klassen, T., Bormann, R., Fernandez, A.: MgH<sub>2</sub> with Nb<sub>2</sub>O<sub>5</sub> as additive for hydrogen storage: chemical, structural and kinetic behavior with heating. *J Acta Mater.* **54**(1), 105–110 (2006)
- Schimmel, H.G., Huot, J., Chapon, L.C., Tichelaar, F.D., Mulder, F.M.: Hydrogen cycling of niobium and vanadium catalyzed nanostructured magnesium. *J Am Chem Soc.* **127**(41), 14348–14354 (2005)
- Mandal, T.K., Sebastian, L., Gopalakrishnan, J., Abrams, L., Goodenough, J.B.: Hydrogen uptake by barium manganite at atmospheric pressure. *Mater Res Bull.* **39**(14–15), 2257–2264 (2004)
- Rahman, M.W., Livraghi, S., Dolci, F., Giamello, E., Baricco, M.: Hydrogen sorption properties of ternary Mg–Nb–O phases synthesized by solid–state reaction. *Int J Hydrog Energy.* **36**, 7932–7936 (2011)
- Rahman, M.W., Castellero, A., Enzo, S., Livraghi, S., Giamello, E., Baricco, M.: Effect of Mg–Nb oxides addition on kinetics of hydrogen storage in MgH<sub>2</sub>. *J Alloys Compd.* **509S**, S438–S443 (2011)
- Friedrich, O., Sanchez-Lopez, J.C., Lopez-Cartez, C., Klassen, T., Bormann, R., Fernandez, A.: Nb<sub>2</sub>O<sub>5</sub> “pathway effect” on hydrogen sorption in Mg. *J Phys Chem B.* **110**(15), 7845–7850 (2006)
- Norin, R., Arbin, C., Nolander, B.: Note on the phase composition of MgO–Nb<sub>2</sub>O<sub>5</sub> system. *Acta Chem Scand.* **26**(8), 3389–3390 (1972)
- Joy, P.A., Sreedhar, K.: Formation of lead magnesium niobate perovskite from niobate precursors having varying magnesium content. *J Am Ceram Soc.* **80**(3), 770–772 (1997)
- Goo, E., Yamamoto, T., Okazaki, K.: Microstructure of lead–magnesium–niobate ceramics. *J Am Ceram Soc.* **69**, C188–C190 (1986)
- Wang, H.C., Schulze, W.A.: The role of excess magnesium oxide or lead oxide in determining the microstructure and properties of lead magnesium niobate. *J Am Ceram Soc.* **73**(4), 825–832 (1990)
- Butcher S.J., Relaxor ferroelectricity in (Pb<sub>x</sub>Ba<sub>1-x</sub>)(Mg<sub>1/3</sub>Nb<sub>2/3</sub>)O<sub>3</sub> ceramics, Ph.D. thesis, University of Leeds, 1989
- Swartz, S.L., Shrout, T.R.: Fabrication of perovskite lead magnesium niobate. *Mater Res Bull.* **17**(10), 1245–1250 (1982)
- Saha, D., Sen, A., Maiti, H.S.: Solid–state synthesis of precursor MgNb<sub>2</sub>O<sub>6</sub> for the preparation of Pb(Mg<sub>1/3</sub>Nb<sub>2/3</sub>)O<sub>9</sub>. *J Mater Sci Lett.* **13**, 723–724 (1994)
- Sreedhar, K., Mitra, A.: Formation of lead magnesium niobate perovskite from MgNb<sub>2</sub>O<sub>6</sub> and Pb<sub>3</sub>Nb<sub>2</sub>O<sub>8</sub> precursors. *Mater Res Bull.* **32**(12), 1643–1649 (1997)
- Zaldo, C., Martin, M.J., Coya, C., Polgar, K., Peter, A., Paitz, J.: Optical properties of MgNb<sub>2</sub>O<sub>6</sub> single crystals: a comparison with LiNbO<sub>3</sub>. *J Phys Condens Matter.* **7**(11), 2249–2257 (1995)
- Raubach, C.W., Santana, Y.V.B., Ferrer, M.M., Longo, V.M., Varela, J.A., Avansi Jr., W., Buzolin, P.G.C., Sambrano, J.R., Longo, E.: Structural and optical approach of CdS@ZnS core–shell system. *Chem Phys Lett.* **536**, 96–99 (2012)
- Cavalcante, L.S., Gurgel, M.F.C., Simes, A.Z., Longo, E., Varela, J.A., Joya, M.R., Pisani, P.S.: Intense visible photoluminescence in Ba(Zr<sub>0.25</sub>Ti<sub>0.75</sub>)O<sub>3</sub> thin films. *Appl Phys Lett.* **90**, 011901–011903 (2007)
- Santos, L.P.S., Cavalcante, L.S., Fabbro, M.T., Beltrán Mir, H., Cordoncillo, E., Andrés, J., Longo, E.: Structural and optical properties of ZnS/MgNb<sub>2</sub>O<sub>6</sub> heterostructures. *Superlattice Microsc.* **79**, 180–192 (2015)
- Ishizumi, A., Kanemitsu, Y.: Luminescence spectra and dynamics of Mn-doped CdS core/shell nanocrystals. *Adv Mater.* **18**(8), 1083–1085 (2006)
- Papulovskiy, E., Shubin, A.A., Terskikh, V.V., Pickard, C.J., Lapina, O.B.: Theoretical and experimental insights into

- applicability of solid-state  $^{93}\text{Nb}$  NMR in catalysis. *Phys Chem Chem Phys.* **15**(14), 5115–5131 (2013)
21. Hong, Y.S., Park, H.B., Kim, S.J.: Preparation of  $\text{Pb}(\text{Mg}_{1/3}\text{Nb}_{2/3})\text{O}_3$  powder using a citrate–gel derived columbite  $\text{MgNb}_2\text{O}_6$  precursor and its dielectric properties. *J Eur Ceram Soc.* **18**(6), 613–619 (1998)
  22. Kim, N.K.: Synthesis chemistry of  $\text{MgNb}_2\text{O}_6$  and  $\text{Pb}(\text{Mg}_{1/3}\text{Nb}_{2/3})\text{O}_3$ . *Mater. Lett.* **32**(2–3), 127–130 (1997)
  23. Camargo, E.R., Kakihana, M., Longo, E., Leite, E.R.: Pyrochlore-free  $\text{Pb}(\text{Mg}_{1/3}\text{Nb}_{2/3})\text{O}_3$  prepared by a combination of the partial oxalate and the polymerized complex methods. *J Alloys Compd.* **314**(1), 140–146 (2001)
  24. Pagola, S., Carbonio, R.E., Alonso, J.A., Fernández-Díaz, M.T.: Crystal structure of  $\text{MgNb}_2\text{O}_6$  columbite from neutron powder diffraction data and study of the ternary system  $\text{MgO}$ – $\text{Nb}_2\text{O}_5$ – $\text{NbO}$ , with evidence of formation of new reduced pseudobrookite  $\text{Mg}_{5-x}\text{Nb}_{4+x}\text{O}_{15-2x}$  ( $1.14 \leq x \leq 1.60$ ) phases. *J Solid State Chem.* **134**(1), 76–84 (1997)
  25. Ananta, S.: Phase morphology evolution of magnesium niobate powders synthesized by solid–state reaction. *Mat Lett.* **58**(22–23), 2781–2786 (2004)
  26. Sun, D.C., Senz, S., Hesse, D.: Crystallography, microstructure and morphology of  $\text{Mg}_4\text{Nb}_2\text{O}_9/\text{MgO}$  and  $\text{Mg}_4\text{Ta}_2\text{O}_9/\text{MgO}$  interfaces formed by topotaxial solid state reactions. *J Eur Ceram Soc.* **26**(15), 3181–3190 (2006)
  27. Dolci, F., Di Chio, M., Baricco, M., Giamello, E.: The interaction of hydrogen with oxidic promoters of hydrogen storage in magnesium hydride. *Mater Res Bull.* **44**(1), 194–197 (2009)
  28. Lutterotti, L., Matthies, S., Wenk, H.-R., Schultz, A.S., Richardson, J.W.: Combined texture and structure analysis of deformed limestone from time-of-flight neutron diffraction spectra. *J Appl Phys.* **81**(2), 594–600 (1997)
  29. Ananta, S., Brydson, R., Thomas, N.W.: Synthesis, formation and characterisation of  $\text{MgNb}_2\text{O}_6$  powder in a columbite-like phase. *J Eur Ceram Soc.* **19**(3), 355–362 (1999)
  30. Yu, Y., Feng, C., Li, C., Yang, Y., Yao, W., Yan, H.: Formation of columbite-type precursors in the mixture of  $\text{MgO}$ – $\text{Fe}_2\text{O}_3$ – $\text{Nb}_2\text{O}_5$  and the effects on fabrication of perovskites. *Mater Lett.* **51**(6), 490–499 (2001)
  31. Costa, A.L., Galassi, C., Roncari, E.: Direct synthesis of PMN samples by spray-drying. *J Eur Ceram Soc.* **22**(13), 2093–2100 (2002)
  32. Thomas, K.N., Torben, R.J.:  $\text{MgH}_2$ – $\text{Nb}_2\text{O}_5$  investigated by in situ synchrotron X-ray diffraction. *Int J Hydrog Energy.* **37**(18), 13409–13416 (2012)
  33. Friedrichs, O., Marti'nez-Marti'nez, D., Guilera, G., Lo'pez, J.C.S., Ferna'ndez, A.: In situ energy-dispersive XAS and XRD study of the superior hydrogen storage system  $\text{MgH}_2/\text{Nb}_2\text{O}_5$ . *J Phys Chem C.* **111**(28), 10700–10706 (2007)
  34. Jin, S.-A., Shim, J.-H., Ahn, J.-P., Cho, Y.W., Yi, K.W.: Improvement in hydrogen sorption kinetics of  $\text{MgH}_2$  with Nb hydride catalyst. *Acta Mater.* **55**(15), 5073–5079 (2007)
  35. Chase M.W. Jr., NIST-JANAF thermochemical tables, 4th Edition, *J. Phys. Chem. Ref. Data, Monogr.*, 9, 1–1951 (1998)
  36. Surrey, A., Nielsch, K., Rellinghaus, B.: Comments on “Evidence of the hydrogen release mechanism in bulk  $\text{MgH}_2$ ”. *Sci Rep.* **7**(44216), 1–4 (2017)
  37. Berlouis, L.E.A., Cabrera, E., Hall-Barentos, E., et al.: Thermal analysis investigation of hydriding properties of nanocrystalline Mg-Ni- and Mg-Fe-based alloys prepared by high-energy ball-milling. *Mater Res.* **16**, 45–57 (2001)
  38. XiangDong, Y., GaoQing, L.: Magnesium-based materials for hydrogen storage: recent advances and future perspectives. *Chin Sci Bull.* **53**, 2421–2431 (2008)
  39. Rahman, M.W.: A proposed kinetic model for hydrogen sorption in  $\text{MgH}_2$ . *Prog React Kinet Mech.* **40**, 402–408 (2015)